

## RESULTS FOR STRANGE PARTICLE PRODUCTION FROM BNL EXPERIMENT E802

Presented by S.G. Steadman, Massachusetts Institute of Technology

### The E802 Collaboration:

T. ABBOTT<sup>k</sup>, Y. AKIBA<sup>e</sup>, D. ALBURGER<sup>b</sup>, D. BEAVIS<sup>b</sup>, R.R. BETTS<sup>a</sup>,  
L. BIRSTEIN<sup>b</sup>, M.A. BLOOMER<sup>i</sup>, P.D. BOND<sup>b</sup>, C. CHASMAN<sup>b</sup>, Y.Y. CHU<sup>b</sup>,  
B.A. COLE<sup>i</sup>, J.B. COSTALES<sup>i</sup>, H.J. CRAWFORD<sup>j</sup>, J.B. CUMMING<sup>b</sup>,  
R. DEBBE<sup>b</sup>, E. DUEK<sup>b</sup>, H. ENGE<sup>i</sup>, J. ENGELAGE<sup>h</sup>, S.Y. FUNG<sup>k</sup>,  
D. GREINER<sup>g</sup>, L. GRODZINS<sup>i</sup>, S. GUSHUE<sup>b</sup>, H. HAMAGAKI<sup>e</sup>, O. HANSEN<sup>b</sup>,  
P. HAUSTEIN<sup>b</sup>, S. HAYASHI<sup>e,1</sup>, S. HOMMA<sup>e</sup>, H.Z. HUANG<sup>i</sup>, Y. IKEDA<sup>f</sup>,  
S. KATCOFF<sup>b</sup>, S. KAUFMAN<sup>a</sup>, K. KITAMURA<sup>d</sup>, K. KURITA<sup>c</sup>, R. LANZA<sup>i</sup>,  
R.J. LEDOUX<sup>i</sup>, M.J. LEVINE<sup>b</sup>, P. LINDSTROM<sup>g</sup>, M. MARISCOTTI<sup>b,2</sup>,  
Y. MIAKE<sup>b,3</sup>, R.J. MORSE<sup>i</sup>, S. NAGAMIYA<sup>c</sup>, J. OLNES<sup>b</sup>, C.G. PARSONS<sup>i</sup>,  
L.P. REMSBERG<sup>b</sup>, M. SARABURA<sup>i</sup>, A. SHOR<sup>b</sup>, P. STANKUS<sup>c</sup>,  
S.G. STEADMAN<sup>i</sup>, G.S.F. STEPHANS<sup>i</sup>, T. SUGITATE<sup>d</sup>, M. TANAKA<sup>b</sup>,  
M.J. TANNENBAUM<sup>b</sup>, M. TORIKOSHI<sup>e</sup>, J.H. VAN DIJK<sup>b</sup>, F. VIDEBAEK<sup>a</sup>,  
P. VINCENT<sup>b</sup>, E. VULGARIS<sup>i</sup>, V. VUTSADAKIS<sup>i</sup>, B. WADSWORTH<sup>i</sup>,  
W.A. WATSON III<sup>b</sup>, H.E. WEGNER<sup>b</sup>, D.S. WOODRUFF<sup>i</sup>, Y. WU<sup>c</sup>, W. ZAJC<sup>c</sup>

<sup>a</sup> Argonne National Laboratory, Argonne, IL 60439

<sup>b</sup> Brookhaven National Laboratory, Upton, NY 11973

<sup>c</sup> Columbia University, New York, NY 10027 and Nevis Laboratories, Irvington, NY 10533

<sup>d</sup> Hiroshima University, Hiroshima 730, JAPAN

<sup>e</sup> Institute for Nuclear Study, University of Tokyo, Tokyo 188, JAPAN

<sup>f</sup> Kyushu University, Fukuoka 812, JAPAN

<sup>g</sup> Lawrence Berkeley Laboratory, Berkeley, CA 94720

<sup>h</sup> Lawrence Livermore National Laboratory, Livermore, CA 94550

<sup>i</sup> Massachusetts Institute of Technology, Cambridge, MA 02139

<sup>j</sup> University of California, Space Sciences Laboratory, Berkeley, CA 94720

<sup>k</sup> University of California, Riverside, CA 92507

<sup>1</sup> JSPS Fellowship for Japanese Junior Scientist

<sup>2</sup> Permanent address: Comision Nacional de Energia Atomica, Buenos Aires, Argentina

<sup>3</sup> On leave of absence from University of Tokyo

### DISCLAIMER

This report was prepared as an account of work sponsored by an agency of the United States Government. Neither the United States Government nor any agency thereof, nor any of their employees, makes any warranty, express or implied, or assumes any legal liability or responsibility for the accuracy, completeness, or usefulness of any information, apparatus, product, or process disclosed, or represents that its use would not infringe privately owned rights. Reference herein to any specific commercial product, process, or service by trade name, trademark, manufacturer, or otherwise does not necessarily constitute or imply its endorsement, recommendation, or favoring by the United States Government or any agency thereof. The views and opinions of authors expressed herein do not necessarily state or reflect those of the United States Government or any agency thereof.



## ABSTRACT

Results are presented for inclusive measurements of  $\pi$ , K, proton and deuteron spectra from 14.5 A-GeV/c Si central collisions with Au targets. Pseudo-rapidity distributions of charged particles from a variety of targets are also shown. Ratios of K to  $\pi$  yields are large and increase with  $p_{\perp}$  for Si+Au collisions.

## 1. INTRODUCTION

The ES02 experiment has been assembled and operational at the Brookhaven National Laboratory AGS for about  $1\frac{1}{2}$  years due to the combined efforts of over 60 scientists from 13 institutions. Not unexpectedly, the 17 graduate students within the collaboration have especially carried the burden of construction and data analysis. Objectives for the experiment include the measurement of strange particle production, in particular, kaon yields, with large phase-space coverage and good event characterization, for collisions of heavy nuclei with a variety of nuclear targets. This large coverage is achieved by rotating the spectrometer, allowing measurements from  $5^{\circ}$  to  $55^{\circ}$  in the laboratory. The momentum range is extended by a series of Čerenkov counters with different thresholds and appropriate segmentation (Fig. 1). The acceptance solid angle of 25 msr is adequate to study pion and (hopefully) kaon interferometry. Inasmuch as the kaon yield for proton-nucleus collisions at AGS energies is typically only 1/20 of the pion yield and the kaon lifetime is short, excellent K- $\pi$  separation and a compact design of 6.5m are essential. This length sets a low-momentum cutoff at 0.5 GeV/c, below which the detection probability for kaons drops rapidly. The momentum acceptance of the spectrometer is shown in Fig. 2. Good event characterization is achieved using the target multiplicity array (TMA), the lead-glass wall (PBGL) that measures transverse energy, and the zero-degree calorimeter (ZCAL).

## 2. EXPERIMENT

Beams of  $^{28}\text{Si}$  and  $^{16}\text{O}$  at 14.5 A-GeV/c are provided at Brookhaven using the dual tandem Van de Graaffs as an injector to the venerable AGS. The limit on mass is given by the velocity of the beam the tandem can deliver for which all electrons may be stripped before injection. A booster synchrotron under construction will have ultra-high vacuum, allowing further acceleration of heavier ions up to Au

before before stripping and injection. Beam rates of typically  $10^5$  Hz are delivered under vacuum to the targets that are 1-3% of an interaction length. A series of thin plastic scintillators in and about the beam establishes the correct beam geometry, the total beam counts, the occurrence of an interaction (seen by loss of charge by the beam particle), and the start time for the time-of-flight to determine particle identification (PID).

The target multiplicity array (TMA), surrounding the target, consists of an array of plastic tubes, operated in the proportional mode, with readout of 3,200 cathode pads. Central collisions are defined to be events that result in charged-particle multiplicities within the upper 7% of this distribution. For nuclear beams, a hardware trigger was derived from the TMA to enhance the data sample for such central collisions to about 50% of the recorded events. These high-multiplicity events also displayed large transverse energy in the PBGL array and low deposited energy in ZCAL (Fig. 3). All the spectra to be shown here will be for such central collisions with  $^{28}\text{Si}$  beams. A discussion of the distributions measured by the PBGL and TMA arrays are presented elsewhere<sup>1</sup>. An analysis of the transverse energy distribution indicates that at AGS energies nuclear stopping (degradation of beam energy below pion production threshold) for the nuclear beams is achieved already for nuclear targets as thick as Ag. Heavier targets have a similar transverse energy distribution at maximum energies.

Particle tracking within the spectrometer is provided by two sets (T1 and T2) of multi-plane drift chambers before and two sets (T3 and T4) after a large aperture (25 msr) dipole magnet. The electronic readout by Fastbus multi-hit TDC's provides for the high multiplicity of measured events (mean $\approx$ 2, range $<$  6 for good tracks behind the magnet) in central collisions at forward angles. Manual scanning of over 100 events indicates that the algorithm used for track reconstruction is about 85% efficient for the range of momentum and multiplicities of the data shown here. The track reconstruction for a multiplicity 4 event is shown in Fig. 4. Particle identification is provided by a 160 slat plastic-scintillator time-of-flight wall (TOF), with 75 ps ( $1\sigma$ , with slewing correction) timing resolution for pions, a 96 segment aerogel Čerenkov counter (AEROČ), and a 40 segment high-pressure gas Čerenkov counter (GASČ). This last detector has just been installed, thus after the data shown here were collected. The TOF is able to provide good K- $\pi$  separation up to 2.2 GeV/c, sufficient for the particle identification for most of

the data discussed here. A separate array of three Čerenkov vessels with associated tracking chambers and scintillator arrays (ČC) extends the momentum range with PID above 5 GeV/c to the beam momentum, albeit with small solid angle (0.5 msr). The outstanding particle separation obtained with this spectrometer is shown in Fig. 5.

### 3. SELECTED RESULTS

The pseudo-rapidity distribution of charged particles, obtained with the TMA for central collisions of  $^{28}\text{Si}$  with a variety of targets, is shown in Fig. 6. (The kink in the distributions at  $\eta = 0$  is an artifact arising from shadowing by the target.) For the Al target, with similar mass to the  $^{28}\text{Si}$  projectile, the distribution peaks at the nucleon-nucleon center-of-mass angle. For the heavier targets the peak shifts backwards in angle. For Au, it peaks at a center-of-mass angle appropriate for emanation from a system consisting of the projectile and the tube of swept out nucleons (total  $\approx 103$  participants) from central collisions. The spectral distributions presented here are for rapidities near the peak of the distribution, namely for  $1.2 < Y < 1.5$ .

The invariant cross sections for pions and kaons within this rapidity interval are shown in Fig. 7 as a function of transverse mass  $m_{\perp} = \sqrt{p_{\perp}^2 + m_0^2}$  for centrally gated Si+Au collisions. These spectra have an overall arbitrary normalization factor and the error bars represent statistical uncertainties only. Additional systematic errors of the order of 10% may be present due to uncertainties in acceptance corrections and run-to-run normalizations; these effects are currently under evaluation. One sees that the spectral distributions are well described as being exponential in  $m_{\perp}$ , with common slopes: such  $m_{\perp}$  scaling would be characteristic of emanation from a thermal source. The exponential lines drawn on Fig. 7 are illustrative only and are not fits to the data. Slope parameters are about 170 MeV.

Results for protons in the same rapidity interval and deuterons in a nearby rapidity interval are shown in Fig. 8. The protons show a similar exponential dependence on  $m_{\perp}$ , but with a larger slope parameter of about 240 MeV. For the same rapidity interval the coalescence model for deuteron production<sup>2</sup> predicts that, if the proton spectra scale in  $m_{\perp}$ , the deuteron spectra should scale with a similar slope. Further analysis of these results within the framework of hydrodynamic and coalescence models is in progress.

## 4. DISCUSSION

The LUND model event generator FRITIOF<sup>3</sup> has been tuned to reproduce inclusive pion distributions in p-p and p-Pb collisions at AGS energies. In the fragmentation function  $f(x, m_{\perp}) = [(1-x)^a/x] e^{-(bm_{\perp}^2/x)}$ , the parameters  $a$  and  $b$  were chosen to be 1.0 and 0.4, respectively, and the  $\sigma$  parameter, which scales the momentum transfer between strings, was set to 0.55. These small changes from the normal parameter set result in excellent fits to pion and proton spectra. Comparisons of these Monte-Carlo model predictions for central Si+Au collisions are shown in Fig. 9 as a function of  $p_{\perp}$ . All four FRITIOF curves were multiplied by a single normalization constant to match the pion data. In Fig. 10 these measured K/ $\pi$  ratios relative to FRITIOF predictions are shown compared with ratios extracted from published p-p and p-Pb data at AGS energies<sup>4</sup>. These published data include ratios of invariant cross sections measured at central rapidities as well as ratios of laboratory cross sections measured at laboratory angles above  $\approx 5^{\circ}$ . One sees that the measured ratios for  $K^+$  to  $\pi^+$  for p-p and p-Pb collisions scale approximately with  $p_{\perp}$ , consistent with the FRITIOF predictions. The approximate  $m_{\perp}$  scaling of the Si+Au cross sections lead to large increases in the K/ $\pi$  ratios with increasing  $p_{\perp}$ . The integrated K/ $\pi$  ratio is dominated by the low  $p_{\perp}$  part of the spectra, and is  $\approx 20\%$  for  $K^+/\pi^+$  and 5-6% for  $K^-/\pi^-$  in this rapidity interval. For p-Pb collisions, the integrated  $K^+/\pi^+$  ratio is 10% and the  $K^-/\pi^-$  ratio is  $\approx 3\%$ .

Finally, the slope parameter for central Si+Au $\rightarrow$ p+X is shown as a function of rapidity in Fig. 11. For a relativistic isotropic thermal source the slope parameter should scale as  $1/\cosh(Y - Y_0)$  with rapidity. Such an illustrative curve is shown on Fig. 11. The comparison seems good at larger rapidities (forward angles) but seems poorer at lower rapidities, perhaps due to contributions in the proton spectra at these back angles from spectator protons. Analysis of recently acquired data will allow a similar comparison to be made for pion production, which would not suffer from the spectator contribution.

## 5. SUMMARY

Inclusive spectra of invariant cross sections for  $K^{\pm}$ ,  $\pi^{\pm}$ , and protons from 14.5 A-GeV/c <sup>28</sup>Si central collisions with Au targets show an exponential dependence on

$m_{\perp}$  for rapidity intervals near  $Y = 0$  in the participant frame. The pions and kaons show approximate  $m_{\perp}$  scaling as well, namely they have similar slope parameters, which is characteristic of a thermal source. Protons and deuterons also display exponential spectra in  $m_{\perp}$ , but with different slopes. The slope parameters for the protons show a dependence on rapidity in the forward region characteristic of an isotropic thermal (fireball) source, and the peak in the pseudo-rapidity distribution for all charged particles occurs at a rapidity appropriate for the participant system defined by the collision geometry. The measured  $K^+/\pi^+$  and  $K^-/\pi^-$  ratios are much larger than ratios measured for p-p and p-Pb collisions at similar AGS energies. Data are available for other targets and for  $^{16}\text{O}$  and proton projectiles. A goal of the experiment is to provide a correlation analysis to determine source sizes; a preliminary analysis is underway.

This work was supported in part by the U.S. D.O.E. under contract with ANL, BNL, Columbia University, LBL, MIT and U.C. Riverside, by NASA under contract with University of California and by the U.S.-Japan High Energy Physics collaboration treaty.

## REFERENCES

- 1) L. Remsberg et. al., *Z. Phys.* C38 35 (1988); T. Abbott et. al., *Phys. Lett.* B197 285 (1987).
- 2) A. Schwarzschild and Č. Zupanič, *Phys. Rev.* 129, 854 (1963).
- 3) B. Andersson, G. Gustafson, G. Ingelman and T. Sjostrand, *Phys. Rep.* 91 31 (1983).
- 4) J. Eichten et. al., *Nucl. Phys.* B44 333 (1972); J.V. Allaby et. al., CERN 70-12 (April 1970), Proc. 4<sup>th</sup> Int. Conf. High Energy Collis., Oxford, UK 85 (1972); U. Becker et. al., *Phys. Rev. Lett.* 31 1731 (1976); A.N. Diddens et. al., *Nuov. Cim.* 31 961 (1964); G.J. Marmer et. al., *Phys. Rev.* 179 1294 (1969); W.F. Baker et. al., *Phys. Rev. Lett.* 7 101 (1961); Y. Raychardhuri, Ph.D. Thesis (unpublished); Y. Makdisi, private communication).

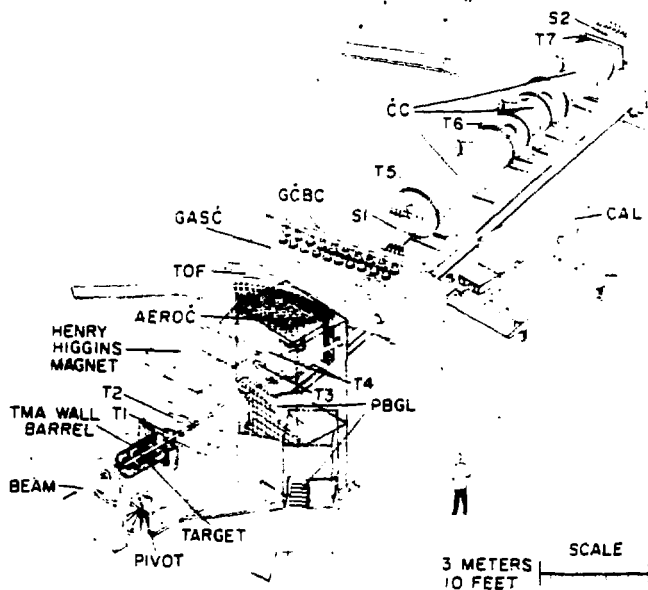


Fig. 1: E802 single arm spectrometer and event characterization detectors.

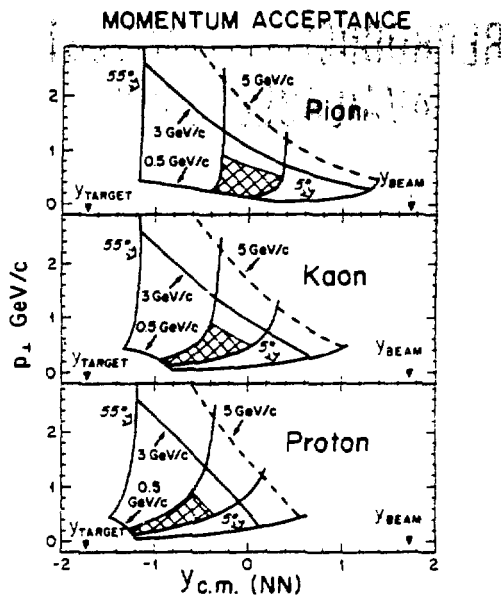


Fig. 2: Acceptance in rapidity vs.  $p_{\perp}$ . The cross hatched regions indicate phase space where data is presented at this conference. Particle identification limits are indicated in the upper panel.

REPRODUCED FROM BEST  
AVAILABLE COPY



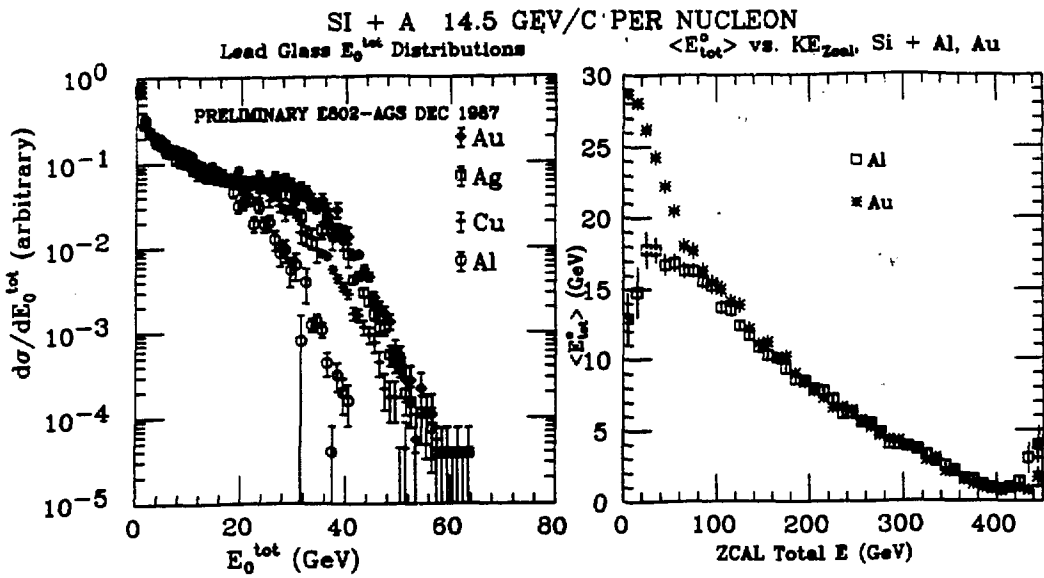


Fig. 3: Left panel: PBGL energy distributions for Si+Au, Ag, Cu and Al collisions. Right panel: correlation between PBGL and ZCAL energies for Si+Al and Si+Au.

REPRODUCED FROM BEST  
AVAILABLE COPY

Fig. 4: Multiplicity 4 event reconstructed through the spectrometer.

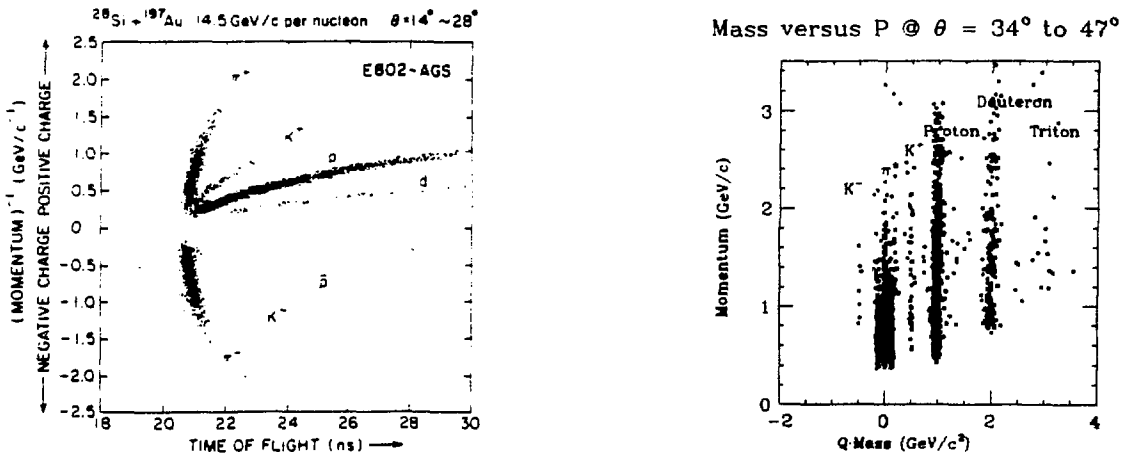


Fig. 5: Particle identification of the E802 spectrometer, (left) scatter plot in time-of-flight vs  $1/p$ , (right) mass vs  $p$ .

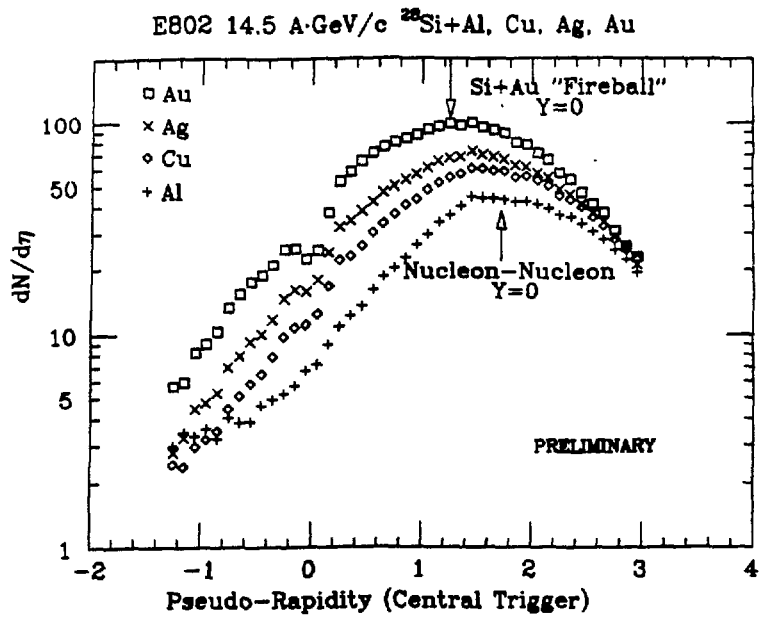


Fig. 6: TMA charged particle multiplicity  $dN/d\eta$  distributions for central Si+Au, Ag, Cu and Al.

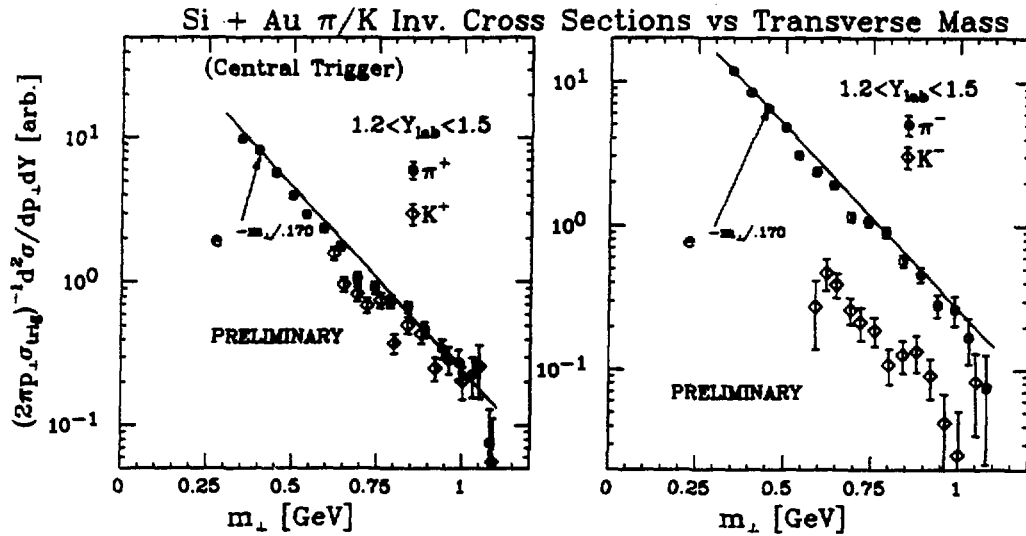


Fig. 7: Invariant cross sections vs  $m_{\perp}$  for central Si+Au  $\rightarrow \pi^{\pm}$  and  $K^{\pm}$ . Exponential lines guide the eye and are not fits. Units are arbitrary.

Si + Au Prot. and Deut. Cross Sections

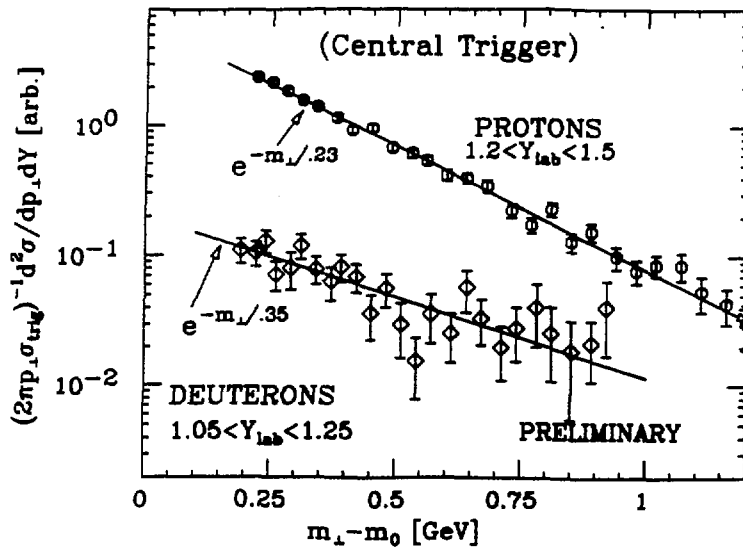


Fig. 8: Invariant cross sections vs  $m_{\perp} - m_0$  for central  $\text{Si} + \text{Au} \rightarrow p + X$  and  $d + X$ . Exponential lines guide the eye and are not fits.

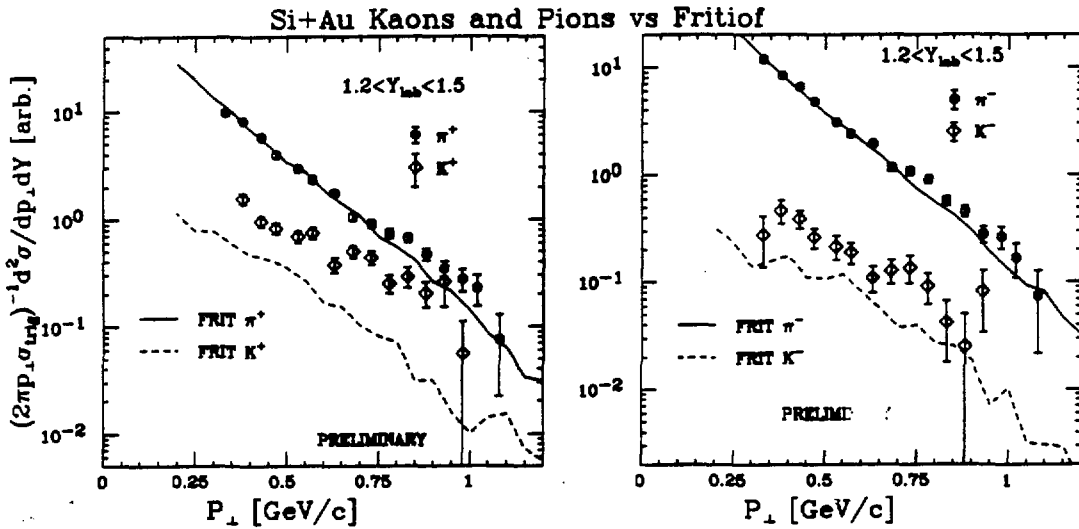


Fig. 9: Invariant cross sections vs  $p_{\perp}$  for central  $\text{Si} + \text{Au} \rightarrow \pi$  and  $K$ , compared to FRITIOF.

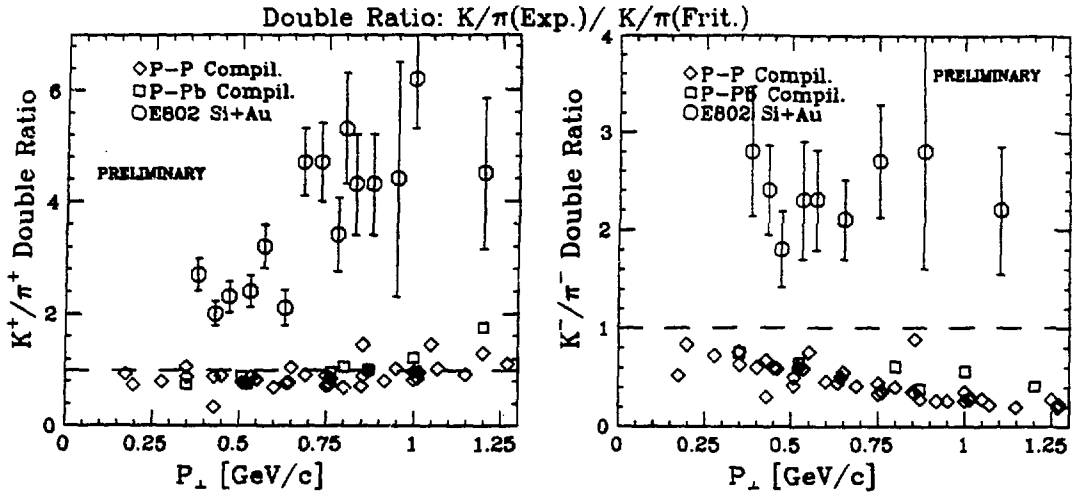


Fig. 10: Double ratio of experimental  $K/\pi$  yields to that of FRITIOF, vs  $p_{\perp}$ .

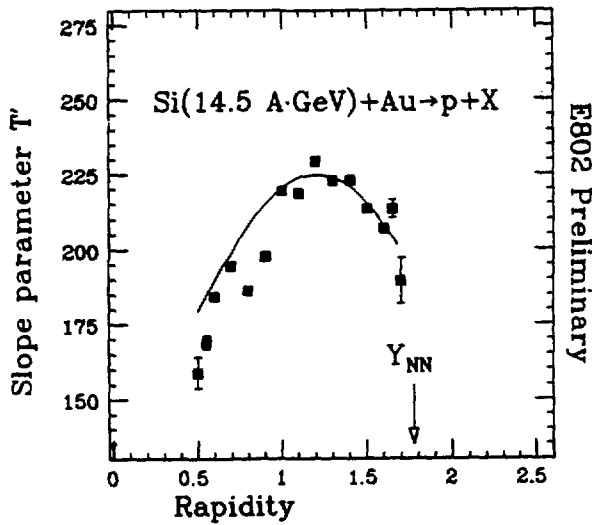


Fig. 11: Slope parameter vs rapidity for central  $Si+Au \rightarrow p+X$ . The curve is  $T' = \frac{225}{\cosh(Y-1.2)}$ ; see text.